On a rough Godunov scheme.

Jean Marie MASELLA [1], Isabelle FAILLE [1] and Thierry GALLOUËT [2]

Abstract - We are interested in the numerical resolution of hyperbolic systems of conservation laws which don't allow any analytical calculation and for which it is difficult to use classical schemes such as Roe's scheme. We introduce a new finite volume scheme called VFRoe. As the Roe scheme, it is based on the local resolution of a linearized Riemann problem. The numerical flux is defined following the Godunov scheme, as the physical flux evaluated at the interface value of the linearized solver. The VFRoe scheme is conservative and consistent without fulfilling any Roe's type condition. Some numerical tests on shock tube problems and two-phase flows problems are presented.

In this communication, we are interested in the numerical resolution of hyperbolic systems of conservation laws which don't allow any analytical calculation. It is well known that due to the nonlinearity of the hyperbolic system, a non-regular solution can appear. Finite volume schemes in conservation form are efficient for tracking such non-regular solutions. A class of such schemes is founded on the resolution of local Riemann problems. The first one was proposed in 1959 by Godunov *[5]* . It consists in solving Riemann problems at each grid interface. The numerical solution is defined by the L^2-projection of the exact solution on the set of cell constant functions. The difficulty to determine the exact solution analytically led many authors to develop schemes based on approximate Riemann solvers (Osher *[14]* , Harten, Lax, Van Leer *[8]*). Such schemes are called Godunov-type schemes. They calculate the numerical solution as the L^2-projection of the solution of the approximate solver on the set of cell constant functions. One of the most popular Riemann solvers currently in use is due to Roe *[15, 16]* . The idea is to replace the non-linear Riemann problem solved at each interface by an approximate linear one. It is defined by a matrix $\tilde{A}(U_L, U_R)$, which depends on the left state U_L and on the right state U_R of the Riemann problem. This matrix, called Roe's matrix, must satisfy the following conditions :

$$\tilde{A}(U_L, U_R) \qquad \textit{is diagonalizable with real eigenvalues} \tag{1}$$

$$F(U_R) - F(U_L) = \tilde{A}(U_L, U_R)\,(U_R - U_L). \tag{2}$$

$$\tilde{A}(U, U) = \frac{\partial F(U)}{\partial U}. \tag{3}$$

The second relation is the well-known Roe condition. It ensures that the Roe scheme is conservative and that the solver recognises isolated discontinuities. Nevertheless, Roe's condition might be very difficult to satisfy in practice. Indeed, in many physical systems such as two phase flow systems *[13, 19, 20]* ,

[1] *Institut Français du Pétrole, 1 à 4, avenue du bois Préau, 92506 Rueil-Malmaison (France), phone number: (+00 33) 1 47 52 73 06, fax number: (+00 33) 1 47 52 70 22.*

[2] *École Normale Supérieure de Lyon, 46 allée d'Italie 69364 Lyon cedex 07 (France), phone number: (+00 33) 4 72 72 80 00, fax number: (+00 33) 4 72 72 80 80.*

turbulent systems *[10]* ..., no analytical calculation is possible because the physical flux is too complicated or not known in closed form.
We propose another scheme called VFRoe which does not require any analytical computation. As Roe's scheme, it uses the solution of a linearized Riemann problem but it does not need to fulfill a Roe type condition to be conservative. Indeed, following Godunov's scheme, the numerical flux is defined as the physical flux computed at the interface solution of the Riemann problem. This scheme is then conservative and consistent. Moreover the VFRoe scheme can be extended to the second order in space with the classical M.U.S.C.L. method (Monotonic Upstream Scheme for Conservation Law) and second order in time with the two-steps Runge Kutta scheme.

After recalling briefly the Godunov scheme and the Roe scheme, we introduce the VFRoe scheme in the first part. Then, in the second part, we study the properties of the scheme. Finally, in the last part some numerical experiments are presented, which show the good behaviour of the VFRoe scheme. First, the scheme is compared to Roe's scheme on some classical tests such as shock tube problems with state near vacuum, double rarefaction waves, double shock waves on the Euler isentropic system, Sod shock tube problem. Secondly, we consider more complex applications namely two-phase flow problems for which analytical computations are difficult.

Notation

Let $p \geq 1$, we consider the Cauchy problem :

$$\begin{cases} \dfrac{\partial U}{\partial t} + \dfrac{\partial F(U)}{\partial x} = 0 \\ U(x,0) = U_0(x) \end{cases} \tag{4}$$

where $U(x,t) \in R^p$, $x \in R$, $t \in R^{+*}$, $U_0(x) \in L^\infty(R, R^p)$ and $F \in C^2(R^p, R^p)$.
The Cauchy problem is said *strictly hyperbolic* if $\frac{\partial F(U)}{\partial U}$ is diagonalizable and have only real and distinct eigenvalues :

$$\lambda_1(U) < \lambda_2(U) < \cdots < \lambda_p(U) \quad \text{where} \quad \lambda_i \in I\!R$$

The set of these states U is called the *hyperbolic domain* of the system (4) and is denoted by $\mathcal{H}$.
We call Riemann problem (*RP* for short), the Cauchy problem (4) with initial condition :

$$\tilde{U}_0(x) = \begin{cases} U_L & if x \leq 0 \\ U_R & if x > 0 \end{cases}$$

and $U_{God}(.; U_L, U_R)$ the entropic solution of the *RP*.
Let consider a regular mesh $M_j = [x_{j-1/2}, x_{j+1/2}]$, with constant length $\Delta x = x_{j+1/2} - x_{j-1/2}$, and let

$I = \bigcup M_j, \forall j \in Z$. Then we define the numerical solution $\{U_j^n \quad \forall j \in Z, n \in N\}$ with

$$U_j^n \approx \frac{1}{\Delta x} \int_{x_{j-1/2}}^{x_{j+1/2}} U(x, t^n)\ dx$$

with $t^n = n\Delta t$ and Δt is the time step determined by a C.F.L. condition of the type $\Delta t \leq CFL \frac{\Delta x}{Sup_I |\lambda_{ij}^n|}$ where λ_{ij}^n is the i^{th} eigenvalue of $\frac{\partial F(U)}{\partial U}(U_j^n)$ and CFL $\in [0, 1]$.

1 The VFRoe scheme

In order to introduce the VFRoe scheme, we first recall Godunov's and Roe's schemes.

1.1 Godunov scheme

The Godunov scheme was introduced by Godunov [5] in 1959. It is founded on the exact resolution of *RP* at each interface of the mesh.
Consider the hyperbolic system (4) and suppose that $U_j^n, \forall j \in Z$ is known. The Godunov scheme constructs the approximation of the numerical solution at time t^{n+1} in two steps. First we solve the *RP* at each interface $x_{j+1/2}$ of the mesh and then we define the numerical solution at time t^{n+1} by L^2 projection of the exact solution on the space of constant cell functions.

$$U_j^{n+1} = \frac{1}{\Delta x} \int_{x_{j-1/2}}^{x_j} U_{God}(\frac{x - x_{j-1/2}}{\Delta t}; U_{j-1}^n, U_j^n)\, dx \ + \ \frac{1}{\Delta x} \int_{x_j}^{x_{j+1/2}} U_{God}(\frac{x - x_{j+1/2}}{\Delta t}; U_j^n, U_{j+1}^n)\, dx$$

In order to have no interaction between two neighboring *RP*, the CFL is restricted to $\frac{1}{2}$. The conservative form of the scheme can be calculated by the integration of the exact solution on every volume $M_j \times [t,\ t + t_{n+1}]$. Since the function $\xi \longmapsto F(U_{God}(\xi; U, V))$ is continuous in $\xi = 0$, we obtain :

$$U_j^{n+1} = U_j^n \ - \ \frac{\Delta t}{\Delta x}\ (F(U_{God}(0; U_j^n, U_{j+1}^n)) \ - \ F(U_{God}(0; U_{j-1}^n, U_j^n))) \tag{5}$$

The numerical flux is defined by $h_{j+1/2}^{God} = F(U_{God}(0; U_j^n, U_{j+1}^n))$. The CFL condition can be relaxed to 1, since only the contribution of the exact solver at the interface is used.
The major drawback of the Godunov scheme is the calculation of the exact solution of each *RP*. This is not always possible in practice and it often requires the use of Newton subroutines, which are costly in computer time. This fact incited many authors *[6, 14, 15]* to develop schemes based on approximate Riemann solvers.

1.2 The Roe scheme

Roe proposed *[15]* a new scheme based on the resolution of a linear Riemann problem (*LRP* for short) :

$$\begin{cases} \dfrac{\partial U}{\partial t} + \tilde{A}(U_L, U_R)\dfrac{\partial U}{\partial x} = 0 \\ U(x,0) = \tilde{U}_0(x) \end{cases} \tag{6}$$

where the matrix $\tilde{A}(U_L, U_R)$ must satisfy :

$$\tilde{A}(U_L, U_R) \qquad \text{has only real eigenvalues and is diagonalizable,} \tag{7}$$

$$F(U_R) - F(U_L) = \tilde{A}(U_L, U_R)\,(U_R - U_L), \tag{8}$$

$$\tilde{A}(U,U) = \frac{\partial F(U)}{\partial U}. \tag{9}$$

These relations are called *"Properties U"* and ensure that the scheme is conservative and recognizes isolated discontinuities. The numerical flux is then defined as :

$$h^{Roe}(U_L, U_R) = \begin{cases} F(U_L) + \tilde{A}^-(U_L, U_R).(U_R - U_L) \\ F(U_R) - \tilde{A}^+(U_L, U_R).(U_R - U_L) \\ \frac{1}{2}\Big(F(U_L) + F(U_R) - |\tilde{A}(U_L, U_R)|.(U_R - U_L)\Big) \end{cases}$$

where

$$\tilde{A}^{\pm}(U_L, U_R) = \frac{1}{2}\,(\tilde{A}(U_L, U_R) \pm |\tilde{A}(U_L, U_R)|)$$

With regards to the previous form of the numerical flux, Roe's scheme can be interpreted as a generalization of the well-known upwind scheme to nonlinear hyperbolic systems. In the framework of Godunov-type schemes *[8]*, Roe's condition (8) can be interpreted as a relation of consistency with the integral form of the nonlinear hyperbolic system (4) :

$$\int_{-\frac{\Delta x}{2}}^{\frac{\Delta x}{2}} U_{Roe}(\frac{x}{\Delta t}; U_L, U_R)\; dx = \frac{\Delta x}{2}\,(U_L + U_R) + \Delta t(F(U_L) - F(U_R))$$

which ensures that the Godunov type scheme obtained is conservative.

The most difficult step of the Roe scheme is the determination of a matrix of linearization. In practice we look for an intermediate state $\tilde{U} \in \mathcal{H}$ such that the Roe matrix is the jacobian of the physical flux in $\tilde{U}$. This method is useful for some systems as Euler's system for perfect gas. Otherwise, Roe suggested to use the method of the vector parameter, which requires an analytical knowledge of the system of conservation laws. In practice, for systems such as two-phase flow systems *[2, 13, 19, 20]*, turbulent systems *[10]*, .., it is not easy to determine a Roe matrix. It can be noticed that some authors *[19, 20]* determined an approximate Roe matrix for such systems, which satisfies Roe's condition up to a certain order of accuracy.

1.3 The VFRoe scheme

We are interested in the discretization of hyperbolic systems for which it is very difficult to use the Godunov scheme or to determine a Roe's matrix. For such systems, we propose a scheme inspired by the Godunov and the Roe schemes but which does not require analytical computations. As Roe's scheme, it uses the solution of a linearized Riemann problem and following Godunov's scheme, the numerical flux is defined as the physical flux computed at the interface solution of the *LRP* :

$$h^{VFRoe}(U_L, U_R) \;=\; F(U_{VFRoe}(0; U_L, U_R)) \tag{10}$$

where $U_{VFRoe}(0; U_L, U_R)$ is the solution of the following *LRP* :

$$\left\{ \begin{array}{l} \dfrac{\partial U}{\partial t} + \tilde{A}(U_L, U_R)\, \dfrac{\partial U}{\partial x} = 0 \\ \qquad U(x, 0) = \tilde{U}_0(x) \end{array} \right. \tag{11}$$

with

$$\tilde{A}(U_L, U_R) \;=\; \frac{\partial F}{\partial U}(\bar{U}) \quad \text{such that} \quad \bar{U} = \bar{U}(U_L, U_R) \in \mathcal{H}. \tag{12}$$

This leads to a conservative scheme for any linearization matrix $\tilde{A}(U_L, U_R)$. Therefore, $\tilde{A}(U_L, U_R)$ can be taken as the jacobian of the physical flux evaluated at a particular state $\bar{U}$. Moreover the flux is consistent for any choice of $\bar{U}$ because :

$$U_{VFRoe}(0; U, U) = U \Longrightarrow h^{VFRoe}(U, U) = F(U)$$

We call this new scheme the VFRoe scheme.

Let us detail the flux expression. Since the jacobian of $F(U)$ is diagonalizable, we deduce that $\tilde{A}(U_L, U_R)$ given by (12) has an eigenvectors base. Consider $\{\tilde{\lambda}_i\}_{i=1,\dots,p}$ the eigenvalues, and $\{\tilde{R}_i\}_{i=1,\dots,p}$ and $\{\tilde{L}_i\}_{i=1,\dots,p}$ the right and left eigenvectors of $\tilde{A}(U_L, U_R)$ such that :

$${}^t\tilde{L}_i.\tilde{R}_j \;=\; \delta_{ij}$$

The solution $U_{VFRoe}(\,.\,; U_L, U_R)$ consists of $p+1$ intermediate states $\{U_i\}_{i=1,\dots,p}$ and can be written :

$$U_{VFRoe}(\frac{x}{t}; U_L, U_R) \;=\; U_L + \sum_{\frac{x}{t} < \tilde{\lambda}_i} \tilde{\alpha}_i\, \tilde{R}_i \quad = U_R - \sum_{\frac{x}{t} > \tilde{\lambda}_i} \tilde{\alpha}_i\, \tilde{R}_i$$

where $\tilde{\alpha}_i = (\alpha_{Ri} - \alpha_{Li}) \;=\; {}^t\tilde{L}_i.(U_R - U_L) \quad \forall\, i = 1, \dots, p$

$$\Longrightarrow U_{VFRoe}(0; U_L, U_R) = U_L + \sum_{i/\tilde{\lambda}_i < 0} \tilde{\alpha}_i\, \tilde{R}_i \;=\; U_R - \sum_{i/\tilde{\lambda}_i > 0} \tilde{\alpha}_i\, \tilde{R}_i$$

The numerical flux is then defined by :

$$h^{VFRoe}(U_L, U_R) \;=\; F(U_{VFRoe}(0; U_L, U_R))$$

and the scheme can be put under the conservative form :

$$U_j^{n+1} = U_j^n - \frac{\Delta t}{\Delta x}(\ h_{j+1/2}^n - h_{j-1/2}^n\ ) \tag{13}$$

where

$$h_{j+1/2}^n \ = \ h^{VFRoe}(U_j^n, U_{j+1}^n).$$

2 Properties of the VFRoe scheme

In the following, we study the stability of the VFRoe scheme in the scalar case. Then, we show that the scheme can suffer from entropy violation problems and an entropy fix is proposed in the vectorial case. Finally, we study the scheme in some particular configurations which show some its drawbacks.

2.1 Stability of the scheme in the scalar case

Suppose $p = 1$, and consider the LRP :

$$\begin{cases} \dfrac{\partial u}{\partial t} + \tilde{\lambda}(u_L, u_R)\, \dfrac{\partial u}{\partial x} = 0 \\ \qquad u(x,0) = \tilde{u}_0(x) \end{cases} \tag{14}$$

Let $f_u(.)$ be the derivative of f with respect to u, then we define :

$$\tilde{\lambda}(u_L, u_R) \ = \ f_u(\bar{u}(u_L, u_R)) \quad \text{such that} \quad \bar{u}(u_L, u_R) \in [Min(u_L, u_R)\, ,\, Max(u_L, u_R)]$$

Let $u_{VFRoe}(\frac{x}{t}; u_l, u_R)$ be the solution of (14). We will show that the choice of $\bar{u}$, is very important and is in direct relation with the stability of the scheme. The following property of convergence can be proven:

Proposition 2.1 *Let $\{u_j^n\}_{\{\forall(j,n)\in(Z,N^*)\}}$ be the sequence produced by the numerical scheme (10), then we can find a subsequence of $\{u_j^n\}$ which converges in $L^\infty(0,T; L^1_{Loc}(R))$ towards a weak solution of (4) if $U(x,0) \in BV(R)$, has a compact support and if we have*

$$\tilde{\lambda}_{j+1/2}\, \frac{f(u_{j+1}^n) - f(u_j^n)}{\Delta u_{j+1/2}^n} \ \geq \ 0 \quad \forall (j,n) \in (Z, N^*) \tag{15}$$

$$\Delta t \ \leq \ \frac{\Delta x}{Sup_{U\in I}|f_u(U)|} \tag{16}$$

__**Proof :**__ The proof is straightforward. Indeed, we can notice that if relation (15) holds, the VFRoe scheme and the Murman-Roe scheme are similar.

Let us however establish the T.V.D. (Harten [6]) and L^∞ stability properties of the scheme under conditions (15) and (16). First the scheme is written under the incremental form :

$$u_j^{n+1} = u_j^n + C_{j+1/2}^{+}\, \Delta u_{j+1/2}^n \ - C_{j-1/2}^{-}\, \Delta u_{j-1/2}^n \tag{17}$$

where $\Delta u^n_{j+1/2} = u^n_{j+1} - u^n_j$, $C^+_{j+1/2} = \dfrac{\Delta t}{\Delta x}\dfrac{f(u^n_j) - h^n_{j+1/2}}{\Delta u^n_{j+1/2}}$ and $C^-_{j+1/2} = \dfrac{\Delta t}{\Delta x}\dfrac{f(u^n_{j+1}) - h^n_{j+1/2}}{\Delta u^n_{j+1/2}}$
Then the scheme is T.V.D. if and only if we have :

$$C^{\pm}_{j+1/2} \geq 0 \quad \text{and} \quad C^+_{j+1/2} + C^-_{j+1/2} \leq 1 \tag{18}$$

For short, we introduce the new variable $\alpha_{j+1/2}$ defined by :

$$\alpha_{j+1/2} = \frac{\tilde{\lambda}^+_{j+1/2}}{|\tilde{\lambda}_{j+1/2}|} \quad \text{where} \quad \tilde{\lambda}^+_{j+1/2} \;=\; Max(0, \tilde{\lambda}_{j+1/2})$$

the VFRoe numerical flux also can be written :

$$h^n_{j+1/2} = \alpha_{j+1/2}\, f(u^n_j) \; + (1 - \alpha_{j+1/2})\, f(u^n_{j+1})$$

The VFRoe scheme is T.V.D. under the following conditions :

$$(1 - \alpha_{j+1/2})\,(f(u^n_j) - f(u^n_{j+1}))\,\Delta u^n_{j+1/2} \;\geq\; 0 \tag{19}$$

$$\alpha_{j+1/2}\,(f(u^n_{j+1}) - f(u^n_j))\,\Delta u^n_{j+1/2} \;\geq\; 0 \tag{20}$$

$$(1 - 2\alpha_{j+1/2})\,\frac{f(u^n_j) - f(u^n_{j+1})}{\Delta u^n_{j+1/2}} \;\leq\; \frac{\Delta x}{\Delta t} \tag{21}$$

$$(19) \text{ and } (20) \Longleftrightarrow \quad \tilde{\lambda}_{j+1/2}\;\frac{f(u^n_{j+1}) - f(u^n_j)}{\Delta u^n_{j+1/2}} \quad \geq 0 \tag{22}$$

$$(21) \Longleftarrow \quad \frac{|f(u^n_j) - f(u^n_{j+1})|}{|\Delta u^n_{j+1/2}|} \leq \frac{\Delta x}{\Delta t} \tag{23}$$

The physical flux f is C^2, so we deduce with the mean value theorem :

$$|f(u^n_{j+1}) - f(u^n_j)| \leq |\Delta u^n_{j+1/2}|\, m_j \quad \forall j \in Z$$

with $m_j = Sup_{u \in I_j} |f_u(U)|$ and $I_j = [min(u^n_{j+1}, u^n_j), max(u^n_{j+1}, u^n_j)]$.
The relation (23) is satisfied under the following stability condition : $\Delta t \leq \frac{\Delta x}{Sup_{U\in I}|f_u(U)|}$ where $I = \bigcup_{j \in Z} I_j$.

<u>Remark :</u> If f_u is positive or negative, the three relations (21) are verified for all $\bar{U}_{j+1/2} \in [min(u^n_j, u^n_{j+1}), max(u^n_j, u^n_{j+1})]$.

Obviously the choice of $\bar{u}_{j+1/2}$ is critical to obtain stability. It is chosen in $\mathcal{H}$ such that relation (15) holds. In practice $\bar{u}_{j+1/2} = \frac{(u^n_j + u^n_{j+1})}{2}$ is often a relevant choice.
If not, we have to consider two cases. First case , if f is convex (or concave) between u^n_j and u^n_{j+1}, we can take $\bar{u}_{j+1/2} = u^n_j$ or $\bar{u}_{j+1/2} = u^n_{j+1}$. One of the two choices satisfies the relation (15). Second case, if f is not convex (or concave) between u^n_j et u^n_{j+1} we should write a research algorithm for a state $\bar{u}_{j+1/2}$ which satisfies relation (15). This case is rare, and in practice hardly ever occurs if the grid is fine enough.

2.2 Sonic entropy correction

It is well-known that schemes based on approximate solver such as the Roe scheme can give non-physical solution due to a lack of dissipation. It is still the case for VFRoe's scheme. Indeed the numerical scheme (13) can give a non physical weak solution, if the exact solution of the *RP* has a rarefaction wave which crosses the interface. Let consider the well-known example of the scalar Bürgers's equation :

$$\begin{cases} \frac{\partial u}{\partial t} + \frac{1}{2}\,\frac{\partial u^2}{\partial x} = 0 \\ u(x,0) = \tilde{u}_0(x) \end{cases}$$

If $u_L = -1$ and $u_R = 1$, the physical solution is a rarefaction wave crossing the interface $x = 0$. For any choice of $\bar{u}(u_L, u_R)$, the VFRoe scheme converges towards a stationary shock misplaced in $x = 0$. Indeed the VFRoe numerical flux is either $h^{VFRoe}(u_L, u_R) = f(u_L)$ or $h^{VFRoe}(u_L, u_R) = f(u_R)$. Because of $f(1) = f(-1)$ the VFRoe scheme gives a stationary shock. This is still the case for Roe's scheme.
Let us consider a *RP* located at the origin defined by the two states U_L and U_R. Suppose that the two states U_{jl} and U_{jr} defined by :

$$U_{jl} = \sum_{i=1}^{j-1} \tilde{\alpha}_i\ \tilde{R}_i \quad \text{and} \quad U_{jr} = U_{jl} + \tilde{\alpha}_j\ \tilde{R}_j$$

are such that :

$$\lambda_j(U_{jl})\ <\ 0 < \ \lambda_j(U_{jr}) \tag{24}$$

where $\lambda_j(U)$ is the j^{th} eigenvalue of $\frac{\partial F(U)}{\partial U}(U)$. The exact solution might consist in a rarefaction wave which crosses the interface $x = 0$.
In order to converge towards the relevant physical solution, we have to modify the VFRoe solver.

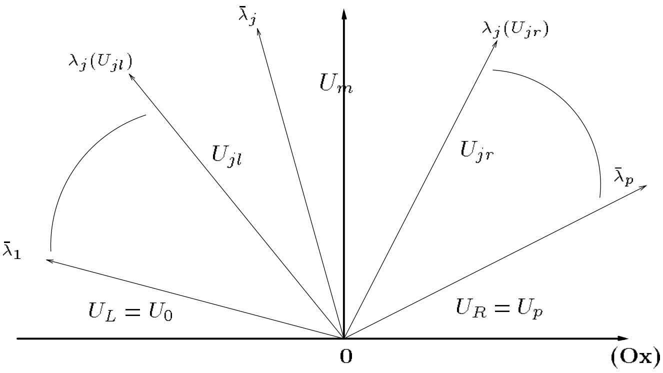

Figure 1: Non parametric entropy correction.

Following the idea of Harten and Hyman *[7]* developed for the Roe scheme, the jump $\tilde{\alpha}_j$ of speed $\tilde{\lambda}_j$ is replaced by two jumps of speed $\lambda_j(U_{jl})$ and $\lambda_j(U_{jr})$ (see fig. 1). The intermediate state U_m is defined by :

$$(\lambda_j(U_{jr}) - \lambda_j(U_{jl}))\ U_m\ = (\lambda_j(U_{jr}) - \tilde{\lambda}_j)\ U_{jr}\ + (\tilde{\lambda}_j - \lambda_j(U_{jl}))\ U_{jl}$$

Some tedious calculations give :

$$U_m\ = U_{jl}\ + \frac{\lambda_j(U_{jr}) - \tilde{\lambda}_j}{\lambda_j(U_{jr}) - \lambda_j(U_{jl})}\ \tilde{\alpha}_j \tilde{R}_j\ = U_{jr}\ - \frac{\tilde{\lambda}_j - \lambda_j(U_{jl})}{\lambda_j(U_{jr}) - \lambda_j(U_{jl})}\ \tilde{\alpha}_j \tilde{R}_j$$

In the case of Roe's scheme, this relation ensures that the scheme is still conservative. For the VFRoe scheme, we can take more simply the state defined by :

$$\tilde{U}_m\ = U_{jl}\ + \frac{{}^t\tilde{L}_j.U_R +^t \tilde{L}_j.U_L}{2}\ \tilde{R}_j\ = U_{jr}\ - \frac{{}^t\tilde{L}_j.U_R +^t \tilde{L}_j.U_L}{2}\ \tilde{R}_j$$

Moreover, in order to obtain less jacobian matrices computation, we propose to verify condition (24) only between the two states U_L and U_R. The modified $U_{VFRoe}(0;U_L,U_R)$ value is then defined :

$$U_{VFRoe}(0;U_L,U_R) = \begin{cases} \tilde{U}_m & \text{if} \quad \exists\, j \in \{1,...,p\} \quad \text{such that} \quad \lambda_j(U_L)\ <\ 0 <\ \lambda_j(U_R) \\ U_L & + \displaystyle\sum_{\tilde{\lambda}_i \leq 0} \tilde{\alpha}_i\ \tilde{R}_i \end{cases}$$

The former correction is used in practice and gives good results. Indeed the main effect of the entropic correction is to "break" the non-entropic stationary shock by introducing some dissipation. So the magnitude of the correction :

$$\frac{{}^t\tilde{L}_j.U_R +^t \tilde{L}_j.U_L}{2}$$

is not of prime necessity. It only has to be not equal to zero.

2.3 Some limits of VFRoe's scheme

Although numerical experiments show the good behavior of the VFRoe scheme (see Section 3), some drawbacks can be noticed. First of all, some negative mass interface states can be computed in some particular cases as shown in the first paragraph. Secondly, some instabilities can appear when there is a change in the sign of an eigenvalue. This last problem is linked to the fact that the flux is not continuous with respect to its arguments when an eigenvalue has a changing sign. This is developed in the second paragraph.

2.3.1 Negative mass interface state

Let us show that for some particular cases, the VFRoe scheme can compute interface states with negative masses. Consider for instance the Euler isentropic equations :

$$\begin{aligned} \frac{\partial \rho}{\partial t} + \frac{\partial \rho\ v}{\partial x} &= 0 \\ \frac{\partial \rho\ v}{\partial t} + \frac{\partial\ (\rho\ v^2\ + P)}{\partial x} &= 0 \end{aligned}$$

with the closure law $P = \rho^\gamma$ where $\gamma > 1$. We define then the *LRP* between the two states U_L and U_R :

$$\begin{cases} \dfrac{\partial u}{\partial t} + \widetilde{A}(U_L, U_R)\ \dfrac{\partial w}{\partial x} = 0 \\ u(x,0) = \tilde{u}_0(x) \end{cases}$$

where the VFRoe matrix $\widetilde{A}(U_L, U_R)$ is given by :

$$\widetilde{A}(U_L, U_R) = \frac{\partial F}{\partial U}(\bar{U}(U_L, U_R)) = \begin{pmatrix} 0 & 1 \\ \bar{c}^2 - \bar{v}^2 & 2\ \bar{u} \end{pmatrix}$$

The sound speed is defined by $\bar{c}^2 = \dfrac{\partial P}{\partial \rho}(\bar{\rho})$.

The solution of the *LRP* is composed of three states. The intermediate state called U_1 is given by :

$$U_1 = U_L + \tilde{\alpha}_1\ \tilde{R}_1 = U_R - \tilde{\alpha}_2\ \tilde{R}_2$$

where $(\tilde{R}_1, \tilde{R}_2)$ are the right eigenvectors of the jacobian matrix and $(\tilde{\alpha_1}, \tilde{\alpha_2})$ are the components of $\Delta U = U_R - U_L$ in the right eigenvectors basis.

If we consider the case where :

$$\tilde{\lambda}_1(U_L, U_R) = 0$$

the intermediate density ρ_1 computed by the VFRoe scheme is written as :

$$\rho_1 = \bar{\rho}(1 - \frac{\Delta v}{2\bar{c}})$$

It is then clear that :

$$\rho_1 > 0 \iff \Delta v \leq 2\bar{c}$$

which is a more restrictive condition than the existence condition of an entropic solution with positive density *[1]* :

$$\Delta v \leq \frac{2}{\gamma - 1}\left(c(\rho_L) + c(\rho_R)\right) \qquad \text{for} \qquad \gamma > 1 \tag{25}$$

where $c(\rho)^2 = \dfrac{\partial P}{\partial \rho}(\rho)$.

Therefore, the VFRoe scheme can lead to a negative intermediate density under the condition (25) and the numerical flux can then not be computed.

2.3.2 Change in the sign of an eigenvalue

Let us consider the case where two states U_L and U_R are such that :

$$\exists i \in \{1, .., p\}\ s.t.\ \tilde{\lambda}_i(U_L, U_R) = O(\epsilon)$$

where ϵ is a small parameter. According to the sign of $\tilde{\lambda}_i(U_L,U_R)$, we can define two interface states $U^\star(U_L,U_R)$ and $U^{\star\star}(U_L,U_R)$:

$$\begin{aligned} U^\star(U_L,U_R) &= U_L + \sum_{j=1}^{i-1} \tilde{\alpha}_j \tilde{R}_j \quad \text{if} \quad \tilde{\lambda}_i(U_L,U_R) > 0 \\ U^{\star\star}(U_L,U_R) &= U_L + \sum_{j=1}^{i} \tilde{\alpha}_j \tilde{R}_j \quad \text{if} \quad \tilde{\lambda}_i(U_L,U_R) < 0 \end{aligned}$$

As the VFRoe flux is given by :

$$h^{VFRoe}(U_L,U_R) = F(U_{VFRoe}(0;U_L,U_R))$$

where $U_{VFRoe}(.;U_L,U_R)$ is the solution of the *LRP* (11), the flux is defined by

$$\begin{aligned} h^{VFRoe}(U_L,U_R) &= F(U^\star(U_L,U_R)) \text{ if } \tilde{\lambda}_i(U_L,U_R) > 0 \\ h^{VFRoe}(U_L,U_R) &= F(U^{\star\star}(U_L,U_R)) \text{ if } \tilde{\lambda}_i(U_L,U_R) < 0 \end{aligned}$$

Assume now, for instance, that $\lambda_i(U_L,U_R) > 0$ and consider a small perturbation on the state U_L, $U_L^{'} = U_L + O(\epsilon)$ such that :

- $\lambda_i(U_L^{'},U_R) < 0$
- $F(U^\star(U_L,U_R)) - F(U^{\star\star}(U_L^{'},U_R)) = O(1)$

Then the numerical fluxes $h^{VFRoe}(U_L,U_R)$ and $h^{VFRoe}(U_L^{'},U_R)$ are such that :

$$h^{VFRoe}(U_L,U_R) - h^{VFRoe}(U_L^{'},U_R) = O(1)$$

although $U_L^{'} = U_L + O(\epsilon)$. The VFRoe flux is therefore not a continuous function with respect to its arguments near states where an eigenvalue can have a change in its sign *[17]* . This non-continuity can sometimes lead to instabilities, in the case of stationary shocks for instance.

3 Numerical experiments

In this section we present some numerical results showing the good behavior of the VFRoe scheme. First shock tube problems on Euler's system and the isentropic Euler's one are shown in order to compare the VFRoe scheme with the classical Roe's scheme. Then we present more complex applications for some two-phase flow systems with boundary conditions.

In the following, $VFRoe$ means the first order VFRoe scheme, and $VFRoe2$ the VFRoe scheme extended to the second order by a MUSCL (Superbee limiter) and Runge Kutta methods.

3.1 Isentropic Euler system

Consider the 1D isentropic Euler's equations :

$$\begin{aligned} \frac{\partial \rho}{\partial t} + \frac{\partial \rho\, v}{\partial x} &= 0 \\ \frac{\partial \rho\, v}{\partial t} + \frac{\partial\, (\rho\, v^2 + P)}{\partial x} &= 0 \end{aligned}$$

with the closure law $P = \beta\, \rho^{\gamma}$ where $(\beta, \gamma) = (1, 1.4)$.

We consider a tube of length 1, the initial discontinuity is located at $x_0 = 0.5$. The mesh is regular and the C.F.L. is set to 0.9 .The exact solution is composed of two pressure waves associated to the eigenvalues $v \pm c$.

Physical variables	ρ_L	v_L	ρ_R	v_R
Test 1	10.00	-8.3	10.0	8.3
Test 2	1.000	0.	10^{-7}	0
Test 3	10.00	$-5.$	10.00	5.
Test 4	10.00	5.	10.00	-5.

Test 1 : Sonic point (fig. 2)

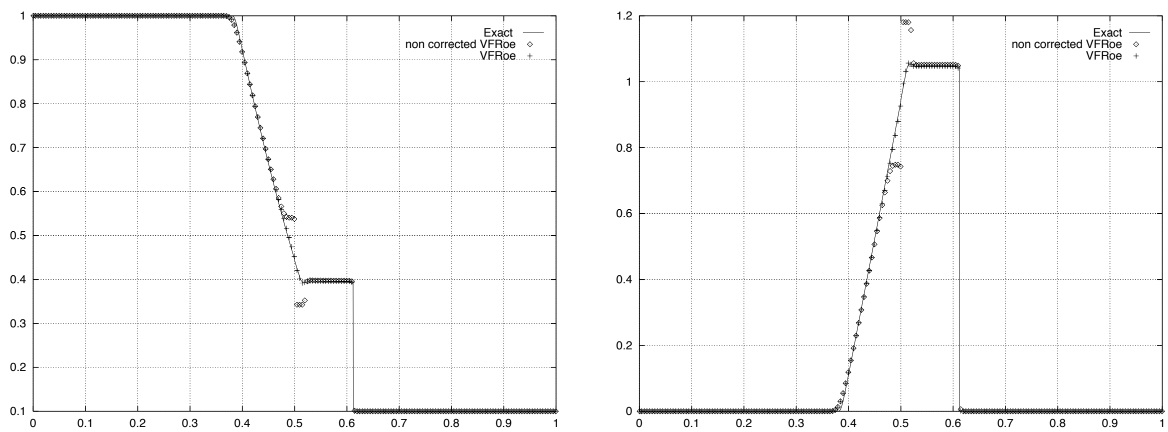

Figure 2: Test 1, density profile ρ (left) and velocity profile v (right) at $t = 0.03s$, 200 cells

We denote by *Non corrected VFRoe* the VFRoe scheme without entropy correction and by *VFRoe* the VFRoe scheme with the entropy correction. The exact solution is composed of a rarefaction wave followed by a shock. The rarefaction wave presents a sonic point (point where $v = c$). The VFRoe scheme, as well as the Roe scheme, gives a stationary shock in the neighborhood of the sonic point. This problem is classic and is due to the loss of diffusion of the scheme at this point. The sonic correction proposed by Harten and Hyman removes this non entropic shock.

Test 2 : State near vacuum (fig. 3)

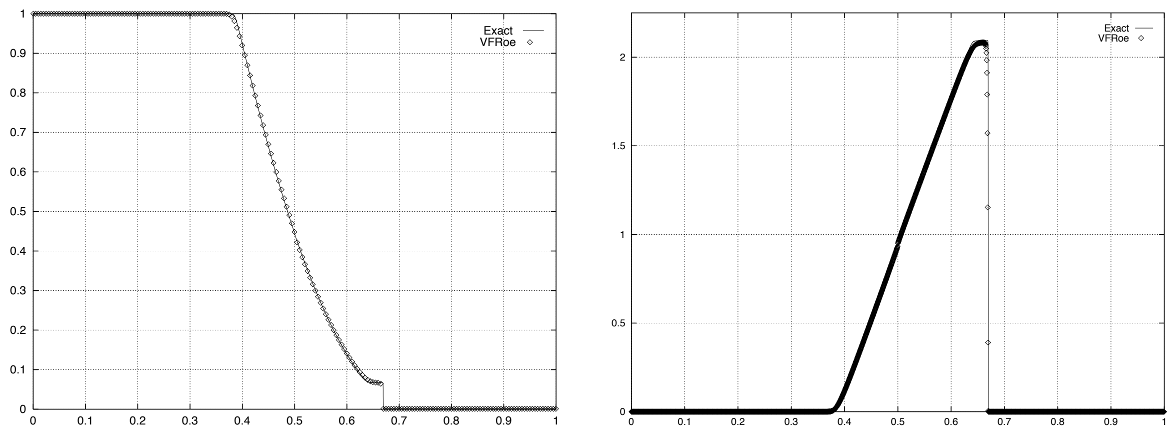

Figure 3: Test 2, density profile ρ (left) and velocity profile v (right) at $t = 0.027s$, 2000 cells

This test is quite difficult because the initial left state is near vacuum. It allows to examine the stability of the scheme. The exact solution is composed of a rarefaction wave (which needs the correction of Harten and Hyman) and of a shock. The speed of the shock might be under-estimated for a coarse grid (this is the case for the Roe scheme and the Godunov scheme *[1]* too). With 2000 cells, the shock is correctly approximated. Moreover the VFRoe scheme preserves the positivity of the density near the shock.

Test 3 : Double rarefaction wave (fig. 4)

In this test, the fluid is pulled to the left and to the right of the tube. The physical solution consists of two rarefaction waves. The intermediate state between the two rarefaction waves is under-estimated, even with $VFRoe2$. This can be a problem when initial states are nearer vacuum. In this case the vacuum can appear on some cells, and the scheme can give a non physical solution *[1]* . This problem is also encountered with the Roe and the Godunov schemes.

Test 4 : Double shock wave (fig. 5)

The fluid is compressed at left and right. Then the exact solution is composed of two shocks. $VFRoe$ and $VFRoe2$ give similar results and are relatively accurate even for a rough grid. Indeed $VFRoe$ is based on a linearized solver, and approximates also accurately the solution composed of shocks.

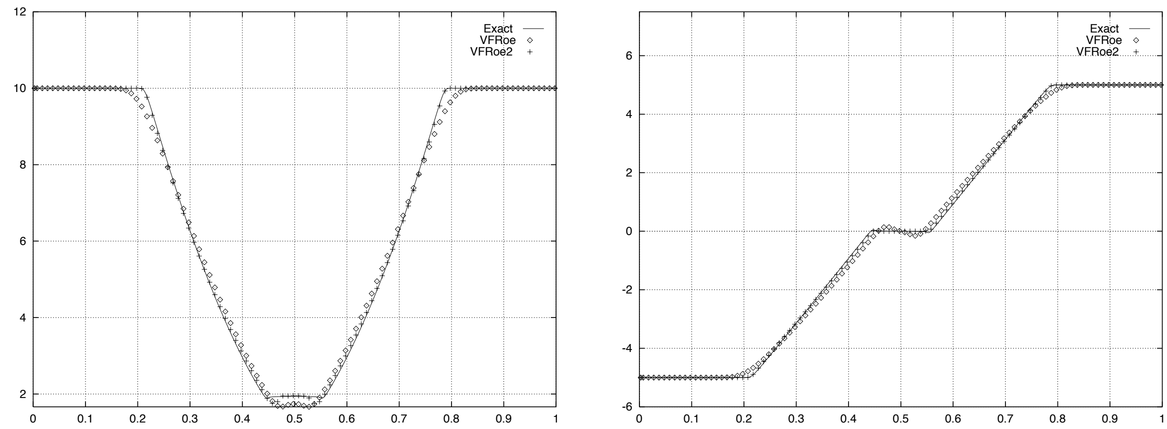

Figure 4: Test 3, density profile ρ (left) and velocity profile v (right) at $t = 0.027s$, 2000 cells

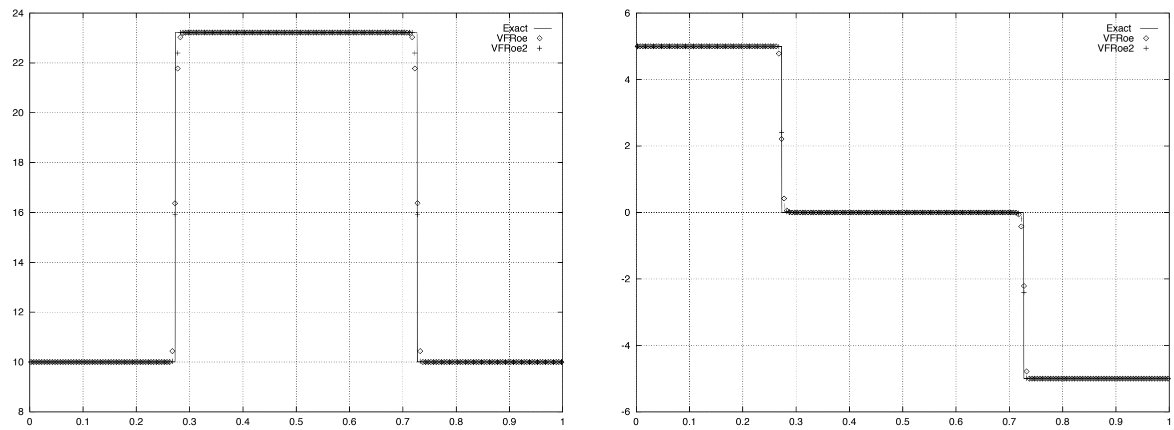

Figure 5: Test 4, density profile ρ (left) and velocity profile v (right) at $t = 0.058s, 200 cells$.

3.2 Euler system

Let a non viscous fluid be governed by the one-dimensional Euler's equation with the perfect gas state law : $P = (\gamma - 1)\,(E - \frac{\rho\, v^2}{2})$ where $\gamma = 1.4$:

$$\begin{aligned} \frac{\partial \rho}{\partial t} + \frac{\partial \rho\, v}{\partial x} &= 0 \\ \frac{\partial \rho\, v}{\partial t} + \frac{\partial\,(\rho\, v^2 + P)}{\partial x} &= 0 \\ \frac{\partial E}{\partial t} + \frac{\partial\, v\,(P + E)}{\partial x} &= 0 \end{aligned}$$

The exact solution is composed of a rarefaction wave associated to $v - c$, followed by a 2-contact discontinuity associated to v and by a 3-shock associated to $v + c$.
The test is due to Sod *[18]* . Initial datas are collected in the following table :

Physical variables	ρ_L	v_L	P_L	ρ_R	v_R	P_R
Test 5	1.00	0.00	10^5	0.125	0.00	10^4

where $(.)_L$ and $(.)_R$ are respectively related to the left and right state of the discontinuity. The length of the tube is 10 and the initial discontinuity is localized at $x_0 = 5$. The C.F.L. is set at 0.9 and the mesh is regular with constant length cell $\Delta x = 0.1$. The space profiles of density, pressure, velocity and Mach number are shown.
Moreover L1-convergence curves on density and velocity are presented at a given time, in order to show the convergence's order of the different schemes VFRoe and VFRoe2. We give the Roe and Roe2 (Roe extented to second order in time and space) schemes as comparison. We define the relative L1-error function at the given time t $E(f_h)(.,t)$ by :

$$E(f_h)(.,t) = \frac{||f(.,t) - f_h(.,t)||_{L1}}{||f(.,t)||_{L1}}$$

where f is the exact solution and f_h the approximated solution. In order to obtain the curves, we used three fine regular grids : 5000 cells, 10000 cells and 20000 cells. The results are represented in log_{10}. The order α is then given by $||f(.,t) - f_h(.,t)||_{L1} = C\;\Delta x^{\alpha}$, where $C \in R^{*+}$.

<u>**Test 5 : Shock tube problem of Sod (fig. 6, 7)**</u>

The flow is subsonic ($M = \frac{v}{c} \leq 1$). We notice that VFRoe gives the three right waves speeds. The contact discontinuity is spreaded (classical behavior due to the C.F.L. which is governed by the pressure waves). The velocity v and the pressure P are constant across the contact discontinuity without apparition of oscillations. VFRoe2 improved the results, namely across the rarefaction wave and the contact discontinuity. The Roe scheme leads to similar results.

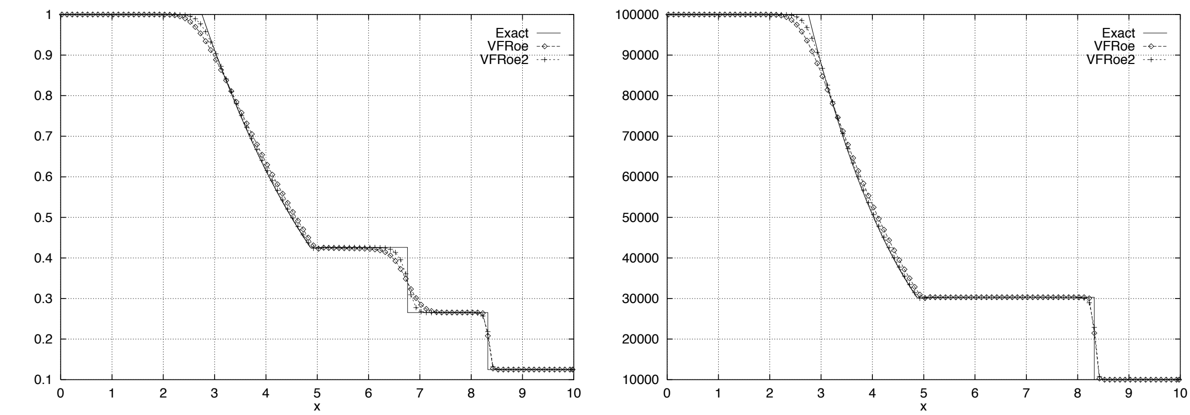

Figure 6: Test 5, density profile ρ (left) and pressure profile p (right) at $t = 0.006s$.

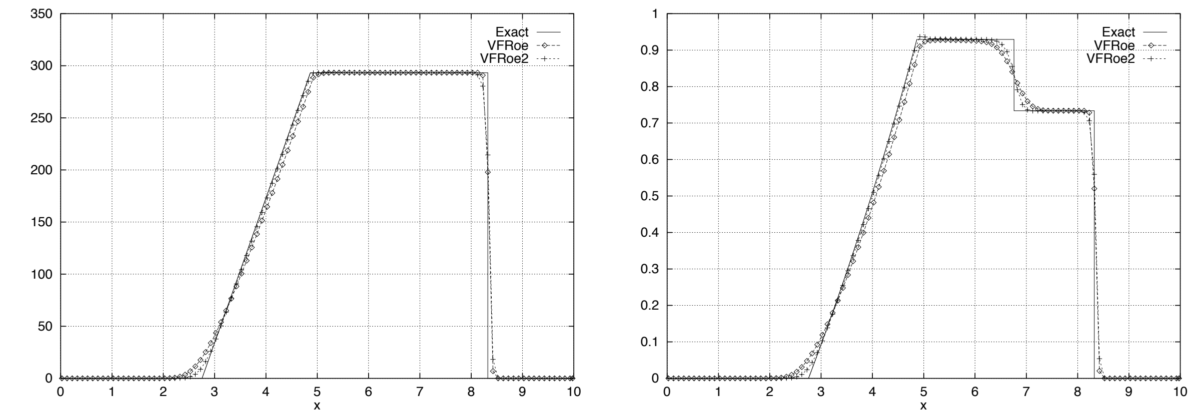

Figure 7: Test 5, velocity profile v (left) and Mach profile $M = \frac{v}{c}$ (right) at $t = 0.006s$.

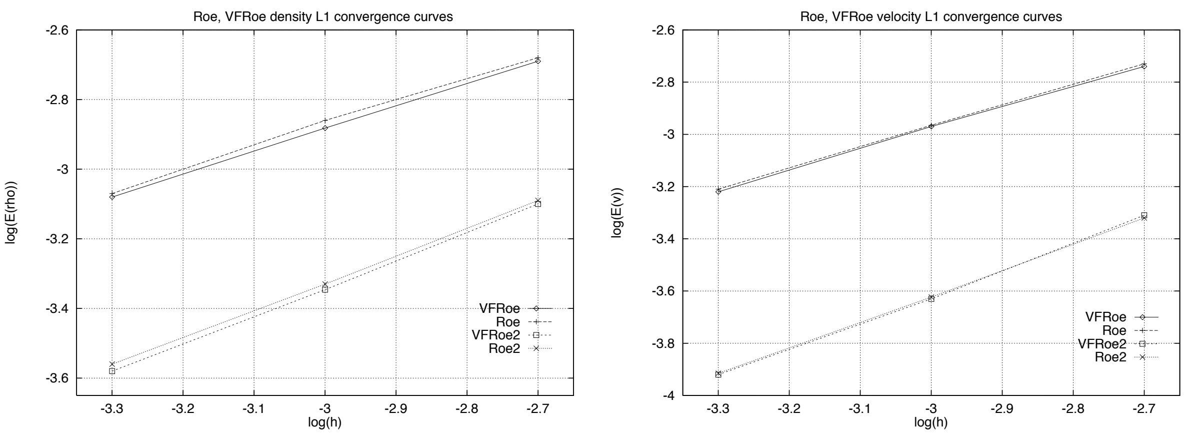

Figure 8: Test 5, density L1-convergence curve (right) and velocity L1-convergence curve (right).

The following results are obtained for the rate of convergence α:

	Density		Velocity
Roe	0.67		0.80
VFRoe	0.67		0.81
Roe2	0.77		0.98
VFRoe2	0.78		1.00

The orders of convergence (at $t = 0.006s$) are below 1. It is a classical result, since the computed solution is non-regular. We notice that, for both schemes VFRoe and VFRoe2 (as for Roe and Roe2), the order of convergence for ρ is less than for v. This could be explained by the fact that the density is not constant through the contact discontinuity as the velocity does. Since schemes are less accurate in the non-regular zone of the solution, the order of convergence could be smaller for the density as for the velocity. However a test for which the density is constant through the contact discontinuity too, shows the same behavior. The results obtained for VFRoe are quite similar as for Roe.

3.3 More complex applications : Two-phase flow in pipelines

We are interested in modeling two-phase (gas-liquid) flow in pipelines. A pipeline is represented as a 1D element of length L with an inclination θ with respect to the horizontal.
We consider two models : the first one is a drift-flux model and the second is a two-fluid model. Both are supposed under isothermal conditions, the unknowns are R_G (resp. R_L) the gas (resp. liquid) volume fraction, v_G (resp. v_L) the gas (resp. liquid) velocity, P the pressure.
The drift flux model is given by the following conservative system of equations :

$$\begin{aligned} \frac{\partial}{\partial t}\rho_G R_G + \frac{\partial}{\partial x}\rho_G R_G v_G &= 0 \\ \frac{\partial}{\partial t}\rho_L R_L + \frac{\partial}{\partial x}\rho_L R_L v_L &= 0 \\ \frac{\partial}{\partial t}(\rho_L R_L v_L + \rho_G R_G v_G) + \frac{\partial}{\partial x}(\rho_L R_L v_L^2 &+ \rho_g R_G v_G^2 + P) = T - (\rho_G R_G + \rho_L R_L) g sin\theta \end{aligned}$$

where g is the gravity acceleration, T is the wall friction which is a given function of the unknowns. We denote by x_G the gas mass fraction : $x_G = \frac{\rho_G R_G}{\rho_G R_G + \rho_L R_L}$.
To close the system, the following additional equations are given :

- $R_L + R_G = 1$
- thermodynamical laws that give fluid properties such as density, viscosity...
- a hydrodynamic closure law which links the difference between the two phases velocities ($dV = v_G - v_L$) to the mixture average velocity ($v_M = R_G v_G + R_L v_L$). Its expression is :

$$\Phi(P, T, R_G, V_M, dV) = 0 \tag{26}$$

The two-fluid model is written under the non-conservative system :

$$\begin{aligned}
\frac{\partial}{\partial t}(R_L\rho_L) + \frac{\partial}{\partial x}(R_L\rho_L v_L) &= 0 && (27)\\
\frac{\partial}{\partial t}(R_G\rho_G) + \frac{\partial}{\partial x}(R_G\rho_G v_G) &= 0 && (28)\\
\frac{\partial}{\partial t}(R_L\rho_L v_L) + \frac{\partial}{\partial x}(R_L\rho_L v_L^2 + R_L\Delta_L) + R_L\frac{\partial}{\partial x}(P) &= T_L - T_i - \rho_L R_L g sin(\theta) && (29)\\
\frac{\partial}{\partial t}(R_G\rho_G v_G) + \frac{\partial}{\partial x}(R_G\rho_G v_G^2 + R_G\Delta_G) + R_G\frac{\partial}{\partial x}(P) &= T_G + T_i - \rho_G R_G g sin(\theta) && (30)
\end{aligned}$$

where g is the gravity acceleration. T_L and T_G are the liquid and gas wall friction and T_i is the interfacial momentum exchange term. All are given functions of the unknowns. This two-fluid model is available in the description of stratified flows, then the two terms Δ_L and Δ_G modelize an hydrostatic pressure distribution (for further details see Masella *[13]*). These two terms are numerically important to ensure the hyperbolicity of the two-fluid model on a physical set of admissible states. To close the system, the following additional equations are given :

- $R_L + R_G = 1$
- $\rho_L = \rho_L^0 + \dfrac{P_L - P_L^0}{a_L^2}$, where $a_L \approx 500m/s$ is the velocity of sound in the liquid phase and (ρ_L^0, P_L^0) are given constant.
- $\rho_G = \dfrac{P_G}{a_G^2}$, where $a_G \approx 300m/s$ is the velocity of sound in gas phase.
- P is the interfacial pressure.

For both two-phase flow models presented above, it is difficult to perform analytical calculations. Moreover for the drift flux model, the hydrodynamic closure law (26) can be solved only numerically, there is no analytical expression of the flux as a function of the conservative variables. Therefore, the use of Roe's scheme can not be considered. Since the VFRoe scheme does not require any analytical computation on the model, it is a useful scheme for the numerical discretization of both two-phase flow models.

We are interested in the simulation of transient phenomena induced by variations of boundary conditions starting from an initial steady state. The boundary conditions are : liquid and gas mass flowrates at the inlet and pressure at the outlet. We analyze in the following two physical applications :

- **Test 6** : Increase of upstream gas mass flow rate, on the drift flux model.
- **Test 7** : Transition to one-phase gas, on the two-fluid model.

Test 6 : Increase of upstream gas mass flow rate

We consider the drift flux model. The VFRoe scheme has been implemented using numerical calculations for the jacobian matrix. These calculations show that the jacobian matrix has, most of the time, two

positive eigenvalues and a negative one. The largest and the smallest eigenvalues correspond to "pressure waves" and the middle one to a "void fraction wave".
The tests presented below show the results obtained for an inlet gas mass flowrate increase in a 10km pipeline. The gas mass flowrate at the inlet (x=0km) is doubled in 10s and the liquid mass flowrate is kept constant. Pressure at the outlet (x=10km) is also kept constant. The simulation lasts for 6000s. The numerical scheme used is the VFRoe scheme extended to the second order in space (MUSCL) and time (Runge-Kutta). The cells are of 200m long and the CFL used is 0.4.
The graphs show time evolution of certain quantities at different points in the pipeline.

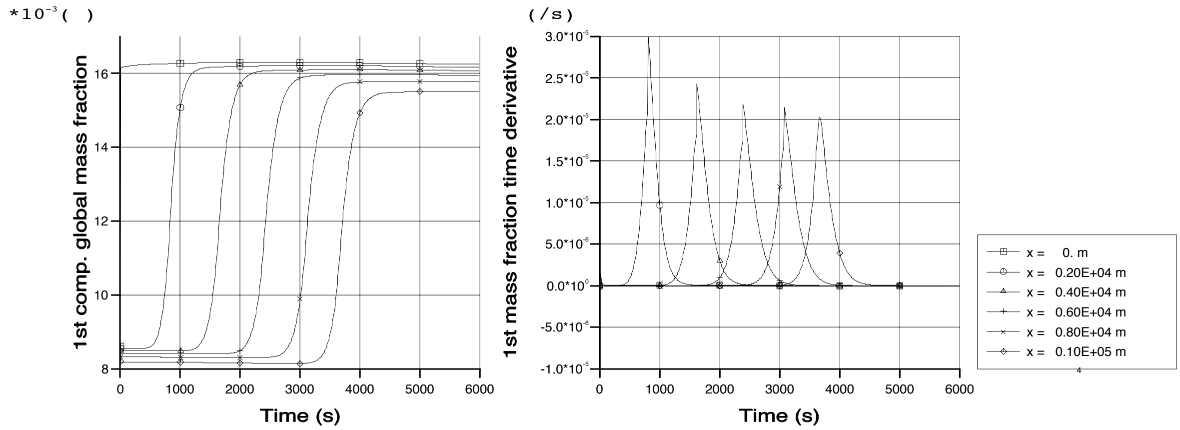

Figure 9: Test 6, pressure P (left) and $\frac{\partial P}{\partial t}$ (right) at $x = 0, 2, 4, 6, 8, 10km$

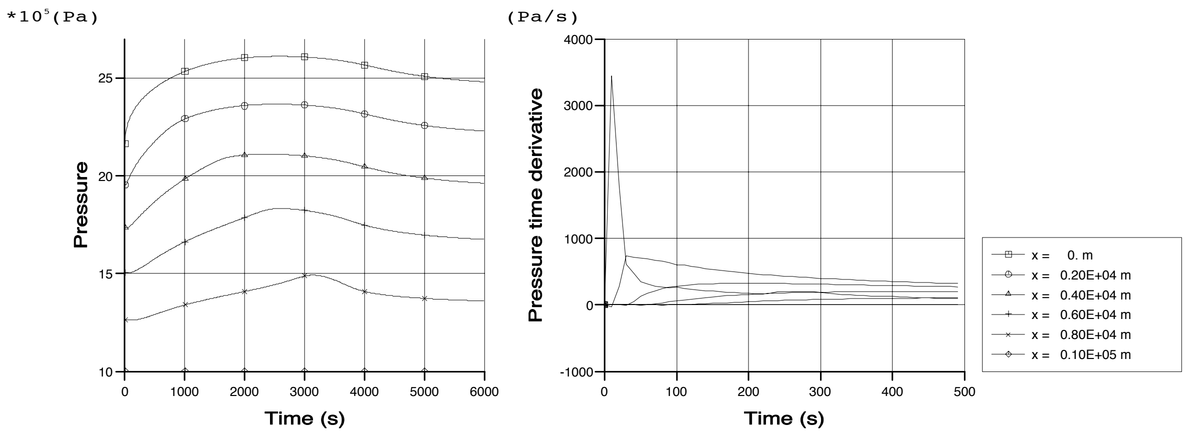

Figure 10: Test 6, gas mass fraction x_G (left) and $\frac{\partial x_G}{\partial t}$ (right) at $x = 0, 2, 4, 6, 8, 10km$

Figure 9 shows that the gas mass flowrate increase generates a pressure wave : it propagates with an average velocity of 80m/s from the inlet to the outlet where it is reflected. It is however rapidly subdued

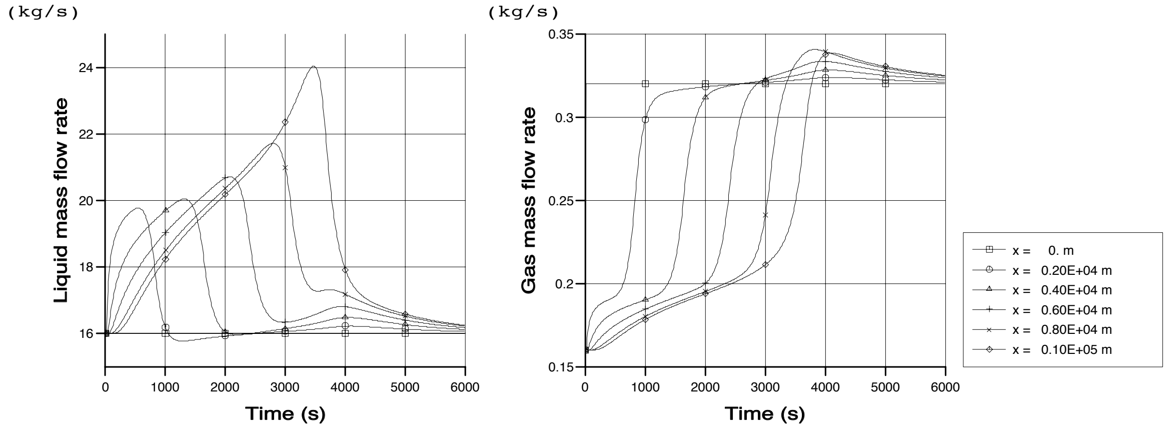

Figure 11: Test 6, gas (left) and liquid (right) mass flowrates at $x = 0, 2, 4, 6, 8, 10km$

due to wall friction. Figure 10 illustrates the propagation of a "void fraction" wave from the inlet to the outlet, with an average velocity of 3m/s. These two waves can also be seen on the mass flowrates curves (fig. 11) where a first modification of the values appears during the first 200 seconds (pressure wave) and a second one which lasts until 6000s ("void fraction wave").
The results obtained with the VFRoe scheme are therefore totally satisfactory.

Test 7 : Transition to one-phase gas, on the two-fluid model

We consider now the two-fluid model. First we can see that the model is non-conservative, but we do not focus on this problem here (for more details see Masella *[13]*). Thanks to the terms Δ_L, Δ_G, it can be shown that the two-fluid model is hyperbolic under the following assumption :

$$\frac{|dv|}{c_m} << 1$$

where c_m is a mean velocity of the sound in the two-phase mixture. The two largest speed are acoustics waves and the two others are void fraction waves.
We consider a pipe $5000m$ long. We use VFRoe scheme extented to the second order in space using minmod limiter. The CFL is fixed to 0.4 and the mesh is regular $\Delta x = 250m$.
At the begining liquid and gas are present in pipe. Then the inlet liquid mass flow rate is decreased to zero in $50s$ (fig. 14). The gas mass flow rate at inlet and the pressure at outlet are kept constant. A void fraction wave of speed $\approx 0.25m/s$ is generated and it propagates from the inlet to the outlet (fig 12). The liquid vanishes in the pipe. The two-phase flow tends towards a one-phase gaz flow. We can see that the two-phase/one-phase transition does not generate any oscillations. A stationary flow is obtained after $10000s$.

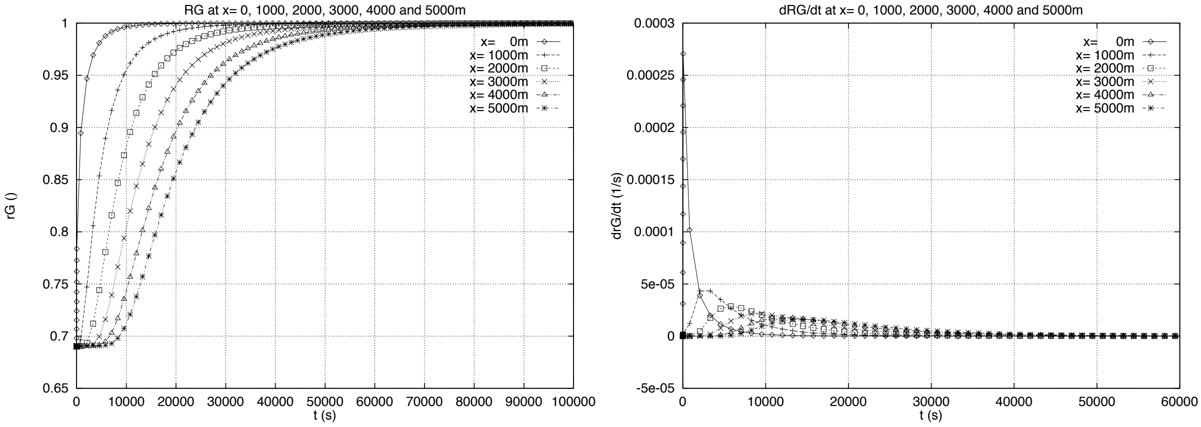

Figure 12: Test 7, gas volumetric fraction R_G (left) and $\frac{\partial R_G}{\partial t}$ (right) time profiles at $x = 0$, 1000, 2000, 3000, 4000, 5000m.

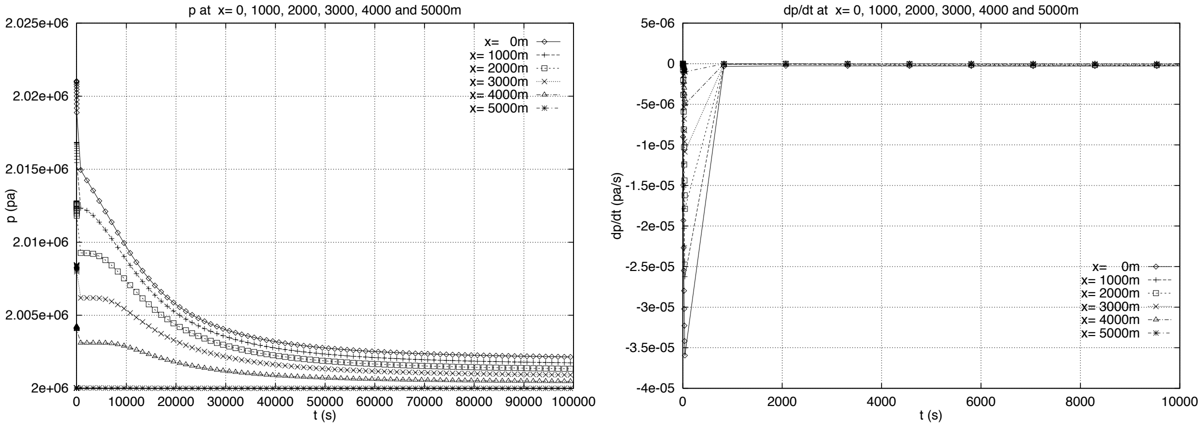

Figure 13: Test 7, pressure P (left) and $\frac{\partial p}{\partial t}$ (right) at $x = 0$, 1000, 2000, 3000, 4000, 5000m.

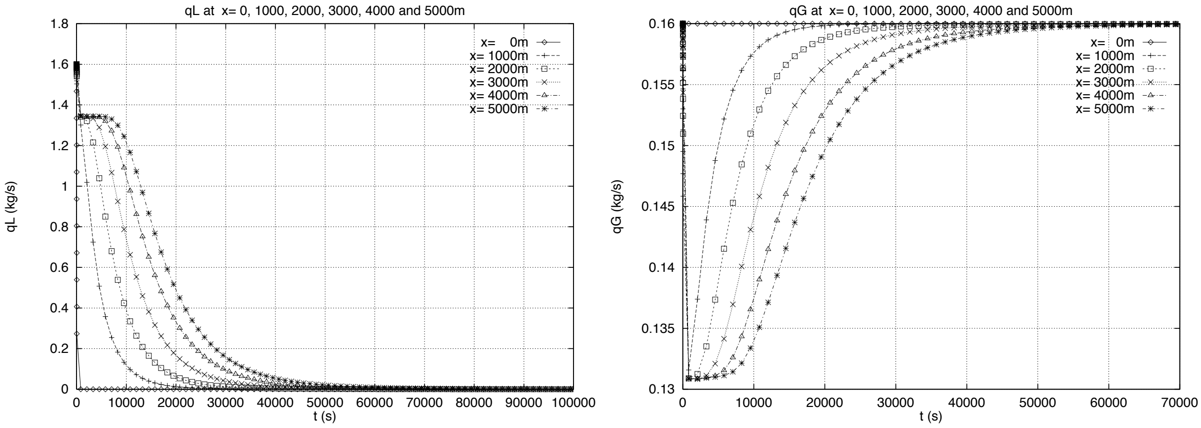

Figure 14: Test 7, liquid $qL = R_L \rho_L v_L$ (left) and gas $qG = R_G \rho_G v_G$ (right) mass-flowrates at $x = 0$, 1000, 2000, 3000, 4000, 5000m.

4 Conclusion

In this paper we proposed a rough Godunov scheme called VFRoe for the discretization of hyperbolic systems which do not allow easy analytical computations. The numerical flux is defined as the conservative form of the Godunov scheme suggests it, substituting the exact solver of a Riemann problem by a rough linearized one. The VFRoe scheme is conservative and consistent. The linearization of the Riemann problem, does not need to fulfill a Roe's type condition, hence the linearized matrix can be given by the jacobian evaluated in a mean state.

In the scalar case, a result of convergence can be proven. Numerically the VFRoe scheme supplies good results. Classical shock tube problems of Sod on the Euler's system, some difficult tests on the Euler's isentropic system as double rarefaction waves with state near vacuum, and some two-phase flow problems with boundary conditions have been experimented. These experiments show the good behavior of the VFRoe scheme. We can also notice that interesting results have been obtained for Euler equations for a Van der Wals gas [9].

As a conclusion, the VFRoe scheme turns out to be an interesting scheme. It gives results in good agreement with Roe's scheme in classical problems. Some limits of VFRoe's scheme can be expected in rare cases (stationary shocks) due to some lack of continuity of the numerical flux. Nevertheless we think that VFRoe's scheme can be very useful in cases where the Roe's scheme is not usable. Since all calculations can be perform numerically, VFRoe's scheme can be implemented for a wide variety of hyperbolic systems, for which any analytical calculation is not easy such as : two-phase flow in a duct, turbulent flows, ...

Acknowledgments - We would like to thank Professor P. L. Roe (*University of Michigan, USA*) for his valuable comments. We are also very grateful to Jean-Marc Hérard (*Laboratoire National d'Hydraulique, EDF Chatou (France)*) for many helpful and stimulating discussions. Also are greatly acknowledged the TACITE group of IFP, within which this work has been done.

References

[1] COMBE L., *Solveur de Godunov pour les équations d'Euler isentropique*, E.D.F. report HE-41/95/008/A, 1995.

[2] FAILLE I., HEINTZE E., *A rough Finite Volume Scheme for Modeling Two-phase Flow in a Pipeline, submitted.*

[3] GALLOUËT T., MASELLA J.M., *Un schéma de Godunov approché*, Note C.R.A.S. Paris, tome 323, Série I p. 77-84, 1996.

[4] GALLOUËT T., *Rough Schemes for Complex Hyperbolic Systems*, Proceedings of the First symposium on Finite Volumes for Complex Applications 15-18 july 1996, p. 5-14, edition Hermes Paris, 1996.

[5] GODUNOV S.K., *A difference method for numerical calculation of discontinuous equations of hydrodynamics*, Math. Sb., vol. 47 p. 217-300, 1959.

[6] HARTEN A., *High resolution schemes for hyperbolic conservation laws*, New York University, rep. DOE/ER/03077-175, 1981.

[7] HARTEN A., HYMAN J.M., LAX P.D., *On finite difference approximations and entropy conditions* , Communication Pure Applied Mathematics, vol. 29 p. 297-322, 1976.

[8] HARTEN A., LAX P.D., VAN LEER B., *On upstream differencing and Godunov schemes for hyperbolic conservation laws*, SIAM review, vol. 25 p. 35-61, 1981 .

[9] BUFFARD T., GALLOUËT T., HÉRARD J.M., *Schémas VFRoe en variables caractéristiques. Principe de base et applications aux cas gaz réels.* Rapport E.D.F. HE-41/96/041/A, 1996.

[10] HÉRARD J.M., *Solveur de Riemann approché pour un système hyperbolique non conservatif issu de la turbulence compressible*, Rapport E.D.F. HE-41/95/009/A, 1995.

[11] LAX P.D , *Hyperbolic systems of conservation laws and the mathematical theory of shock waves*, SIAM Regional Conference series in Applied Mathematics, vol. 11, 1973.

[12] LAX P.D, WENDROFF B., *Systems of conservation laws*, Communication Pure Applied Mathematics, vol. 13 p. 217-237, 1960.

[13] MASELLA J.M, Thesis of the University of Paris VI, in preparation.

[14] OSHER S., *Riemann solvers, the entropy conditions, and difference approximations* , SIAM Journal Numerical Analysis, vol. 21 p. 217-235, 1984.

[15] ROE P.L., *The use of Riemann problem in finite difference schemes*, Lectures notes of physics, vol. 141 p. 354-359, 1980.

[16] ROE P.L., *Approximate Riemann solvers, parameters vectors and difference schemes*, Journal of computational physics, vol. 43 p. 357-372, 1981.

[17] ROE P.L., *personal communication*

[18] SOD G. A., *A survey of several of finite difference methods for systems of nonlinear hyperbolic conservations laws*, Journal of computational physics, vol. 27 p. 1-31, 1978.

[19] SAINSAULIEU L. , *Modélisation, analyse mathématique et numérique d'écoulements diphasiques constitués d'un brouillard de gouttes.*, Thesis of the École Polytechnique, 1991.

[20] TOUMI I. , *Etude du problème de Riemann et construction de schémas numériques type Godunov multidimensionnels pour des modèles d'écoulements diphasiques*, Thesis of the University of Paris VI, 1989.

[21] TRAN H., MASELLA J.M., FERRÉ D., PAUCHON C., *Transient simulation of Two-phase flows in pipes*, submitted.